Journal of the Geological Society, *London*, Vol. **156,** 1999, pp. 943–955. Printed in Great Britain.

Sulphur isotope compositions of sedimentary phosphorites from the basal Cambrian of China: implications for Neoproterozoic–Cambrian biogeochemical cycling

GRAHAM A. SHIELDS[1], HARALD STRAUSS[2], STEPHEN S. HOWE[3] & HENDRIK SIEGMUND[4]

[1]*Centre de la Géochimie de la Surface, ULP-EOST-CNRS, 1 rue Blessig, F-67084, Strasbourg, France (e-mail: shields@elite.u-strasbg.fr)*

[2]*Ruhr-Universität Bochum, Institut für Geologie, D-44780 Bochum, Germany*

[3]*Department of Earth and Atmospheric Sciences, Earth Science 352B, University at Albany, 1400 Washington Avenue, Albany, NY 12222, USA*

[4]*Institut für Geologie und Paläontologie, Universität Tübingen, Sigwartstr. 10, D-72076 Tübingen, Germany*

Abstract: The Meishucun Section (Yunnan Province, South China) is considered to be an important Precambrian–Cambrian boundary section, primarily because of its rich small shelly fossil record. In this article, we report the results of a sulphur isotope study of phosphate-bound sulphate from the Meishucun Section and several correlative sections in South China. Forty clastic, granular phosphorites from Meishucun yield tightly grouped $\delta^{34}S$ values averaging 33‰ (CDT), which agree well with published evaporite data for the lower Cambrian of Siberia and elsewhere. We argue that these strongly positive values reflect the sulphur isotopic composition of ambient seawater, confirming further the existence of uniquely high $\delta^{34}S$ values in the earliest Cambrian oceans. This novel use of trace-sulphate in phosphate to constrain seawater $\delta^{34}S$ represents the first time that sulphate $\delta^{34}S$ data for this period have been given precise biostratigraphic assignments. Superimposed on the overall trend are short-term, stratigraphic variations, which might reflect local variations in the sedimentary and early diagenetic environment. Our data, together with other published data, indicate that seawater sulphate $\delta^{34}S$ rose from low values (15–20‰) during the pre-750 Ma Proterozoic to possibly all-time high values (>32‰) by the earliest Cambrian. We argue that this rise may, in part, relate to increases in the amount of sulphur isotopic discrimination during microbially mediated sulphate reduction as a result of increased sulphide reoxidation. On the other hand, the Neoproterozoic trend to high $\delta^{34}S$ values appears to mirror a trend to decreasing seawater $\delta^{13}C$ towards the Proterozoic–Phanerozoic transition, implying progressive increases in the efficiency of organic carbon recycling, which would normally be coupled with real increases in sulphate reduction on the global scale. We consider that both these changes in biogeochemical cycling derive ultimately from the introduction of macrofauna around this time and, in particular, from the influence of bioturbation on early diagenesis. Precise constraints on S-isotopic evolution during the Neoproterozoic require additional trace sulphate studies.

Keywords: Cambrian, China, S isotopes, seawater, phosphorites.

Over the last few decades there has been a concerted effort to constrain temporal variations in the isotopic composition of seawater around the Proterozoic–Phanerozoic transition. Carbon and strontium isotope studies have significantly improved Neoproterozoic–Cambrian stratigraphic correlation and calibration (Kaufman & Knoll 1995; Brasier *et al.* 1996). By comparison, our knowledge of temporal variations in the sulphur isotopic composition of seawater sulphate has remained largely unaltered since the 1960s when it first became known that the Precambrian–Cambrian transition was accompanied by elevated $\delta^{34}S$ values in seawater, (e.g. Thode & Monster 1965). The aim of this study is to improve constraints on changes in seawater $\delta^{34}S$ during Neoproterozoic–Cambrian time in order to compare this record with the better resolved ^{13}C and $^{87}Sr/^{86}Sr$ records. The establishment of a correctly calibrated sequence of isotopic events and trends will shed light on major changes in the surface environment as well as provide answers to some of the most intriguing questions in animal evolution, such as the origin of metazoans and animal biomineralisation in the Neoproterozoic.

Holser (1977) related the phenomenon of positive $\delta^{34}S$ excursions during the Phanerozoic (Precambrian–Cambrian, mid-Devonian and early Triassic) to the catastrophic influx of ^{34}S-enriched, saline waters from previously restricted basins during transgression. The early Cambrian event was given the name 'Yudomski event' after the rock successions in Siberia where evaporites of this age show uniquely high $\delta^{34}S$ values (Pisarchik & Golubchina 1975; Pisarchik *et al.* 1977; Claypool *et al.* 1980). Strongly positive $\delta^{34}S$ values in evaporite sequences of comparable age in other areas such as southern Iran (Houghton 1980; Strauss & Deb, unpubl. data), Oman (Mattes & Conway Morris 1990), Siberia (Strauss, H. unpubl. data) and India (Strauss & Banerjee 1998) have since confirmed this observation.

The Neoproterozoic record is much more sparse (Fig. 1), making the timing of the late Precambrian rise to high $\delta^{34}S$ particularly difficult to resolve. Strauss (1993) concluded that seawater $\delta^{34}S$ ranged between 15‰ and 20‰ from 1200 Ma to 750 Ma. Data from the Bitter Springs Formation, Amadeus Basin, central Australia and the Redstone River Formation, Mackenzie Mountains Supergroup, northern

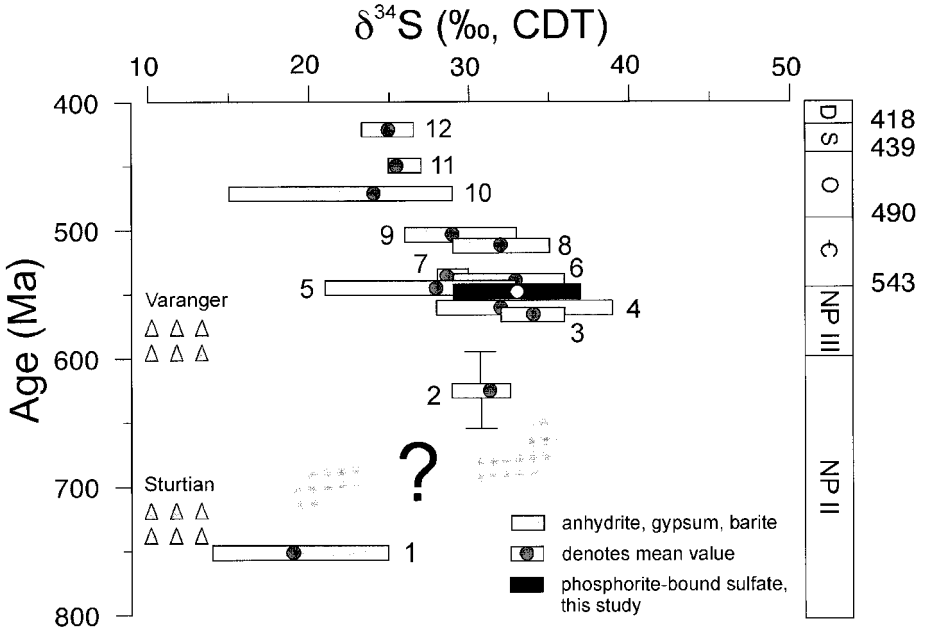

Fig. 1. Sulphur isotopic composition of phosphorite-bound sulphate from Meishucun superimposed on the temporal evolution of seawater sulphate as defined by evaporites (modified after Strauss & Banerjee 1998). 1, Redstone River, Canada; 2, Irecj Basin, Brazil (barite and anhydrite) (Misi & Veizer 1998); 3, Siberia (unnamed Precambrian); 4, Hanseran Formation, India (Strauss & Banerjee 1998); 5, Hormuz Formation, Iran (Houghton 1980); 6, Siberia (lower, lower Cambrian); 7, Desu Series, Iran (Strauss & Deb, unpubl.); 8, Siberia (upper, lower Cambrian); 9, Siberia (lower, middle Cambrian); 10, Northwest Territories, Canada; 11, Williston Basin, USA (Fox & Videtich 1997); 12, Michigan, USA. Other data from Holser *et al.* 1966; Claypool *et al.* 1980; Strauss 1993. NP II and NP III are stratigraphic divisions of the Neoproterozoic.

Canada constrain late, pre-Sturtian $\delta^{34}S$ to below 20‰ (Strauss 1993), but there are few constraints within the vital period from 750 Ma to 540 Ma. This period is one of intermittent glaciation and begins with the Rapitan or Sturtian ice age (*c.* 750 Ma). Data from Brazil (Misi & Kyle 1994; Misi & Veizer 1998) are likely to come from this time window (Fig. 1). These samples come from unit B1 of the Una Group, Irece Basin and lie about 400 m above glacial diamictites of the Bebedouro Formation, which is believed, on chemostratigraphic evidence, to be Sturtian in age (Misi & Veizer 1998). Thirteen samples of sedimentary barite and gypsum yielded $\delta^{34}S$ values between 25‰ and 32‰, with a mean value around 27.7‰. Seven pyrite-free samples yield a mean value of 31‰ which is considered by these authors to correspond more faithfully to ambient seawater. These data and coeval pyrite data (Ross *et al.* 1995; Canfield & Teske 1996) indicate that seawater $\delta^{34}S$ had already risen from the long Proterozoic plateau of low values by the Vendian and was possibly as high or higher than the peak in the early Cambrian (>32‰) between 600 and 550 Ma (Lambert *et al.* 1987; Hall *et al.* 1991; Ross *et al.* 1995). More sulphate data are clearly needed for this time period before firm constraints on the timing of this rise can be made.

Difficulties in resolving the late Precambrian $\delta^{34}S$ rise derive from (1) the lack of suitable evaporite successions in the latest Proterozoic; (2) the inherent difficulty involved in correlating and dating evaporite suites using palaeontology; (3) the influence of non-seawater sources on evaporite $\delta^{34}S$ such as freshwater influx (Pisarchik *et al.* 1977) and sulphate reduction within a closed basin, leading to disparity between evaporite sulphate $\delta^{34}S$ values. In this study, we have taken an alternative approach to constraining seawater $\delta^{34}S$ which involves the measurement of phosphate-bound sulphate. Phosphorite is particularly abundant close to the Precambrian–Cambrian boundary in many parts of the world, especially in Asia (Cook & Shergold 1986; Shields *et al.* 1999). The Meishucun Section, the main focus of our research, was proposed as the global boundary type section (Luo *et al.* 1984) and as such is well known palaeontologically. This article represents the first time that sulphur isotope data from this interval have been presented with such a precise biostratigraphic assignment.

Geological setting

The Sinian–Meishucunian (Neoproterozoic–Cambrian) sedimentary sections of South China (Fig. 2) have been the subject of close scrutiny and controversy ever since the announcement of the Meishucun Section as one of the three candidates for the Precambrian–Cambrian boundary global stratotype in 1983 (Cowie 1985). The Meishucun Section (Kunyang Mine, near Kunming, Yunnan Province) appeared suitable for the role of global stratotype because of the high diversity of pre-trilobitic,

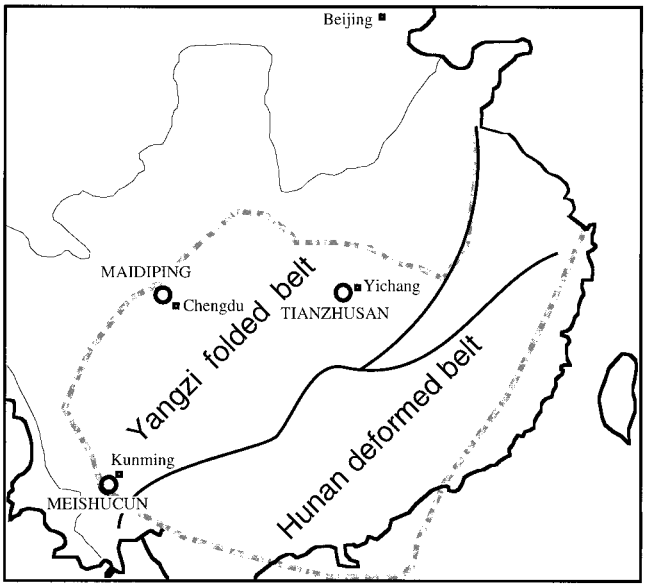

Fig. 2. Map showing the locations of the Meishucun Section, Kunyang Mine, near Kunming, Yunnan Province; Maidiping Section, near Chengdu, Sichuan Province; Tianzhushan Section, West of Yichang, Hubei Province and the limits of the Yangzi palaeogeographic block.

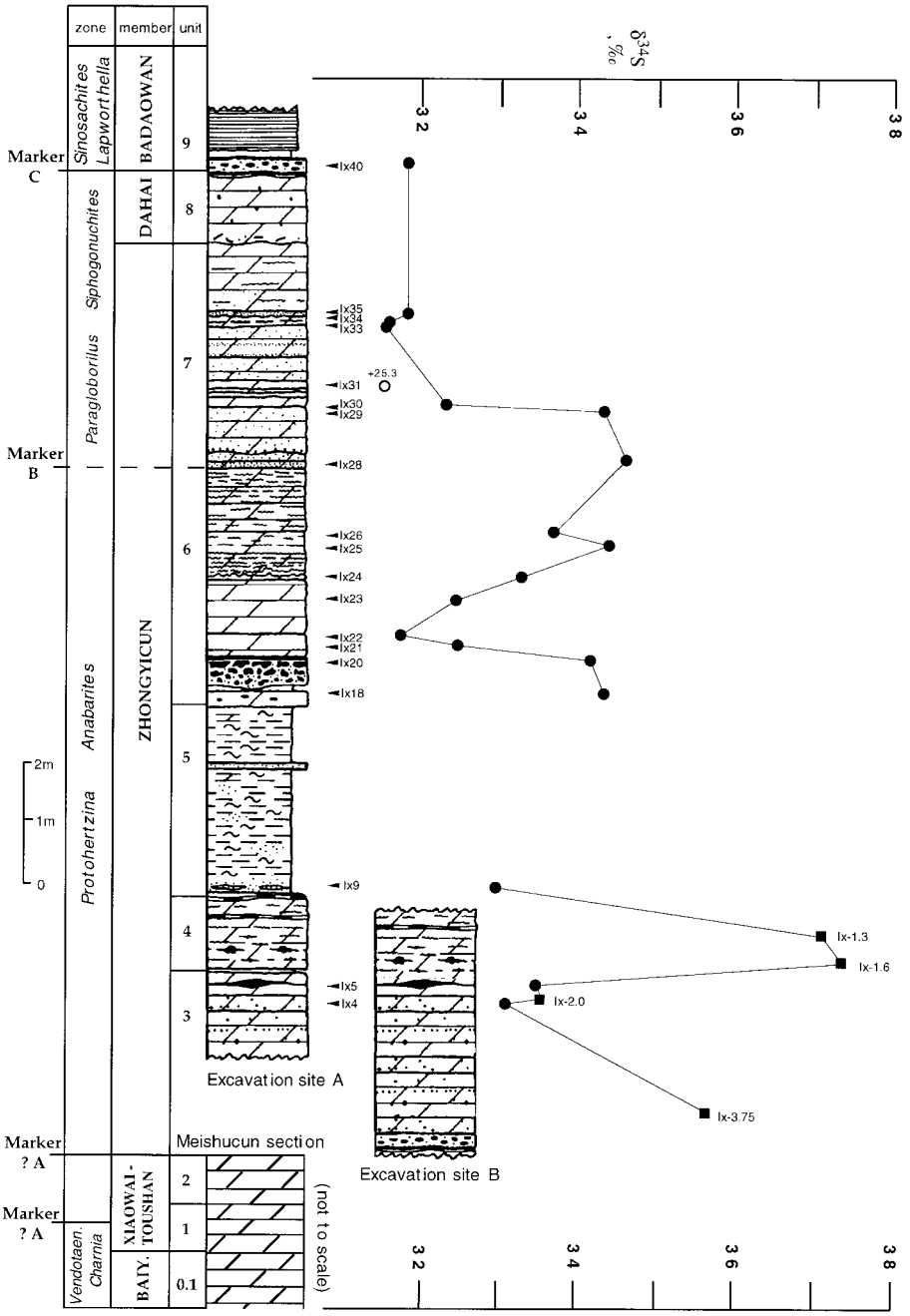

Fig. 3. Integrated stratigraphy of the Meishucun Section. High resolution S isotope data (this study: Table 1) for Meishucun excavation sites A and B (Siegmund 1995) show minor stratigraphic variation with only one significant outlier (Ix 31), which is a phosphatic dolomite.

small shelly fossils (SSF) found there and because these SSFs appear in the middle of the section, suggesting that their sudden appearance may relate to an evolutionary event (Luo *et al*. 1992). A composite profile of the Meishucun section is shown in Fig. 3. Four biostratigraphic marker levels can be widely correlated: Marker 'A' marks the 'first appearance datum' (FAD) of SSFs at Meishucun. Marker 'B' indicates a marked increase in SSF diversity and was the suggested boundary level, supposedly correlative with the base of the Tommotian in Siberia (Rozanov 1984). Marker 'C' corresponds to a profound facies change from evaporitic dolomite to organic-rich siltstone with nodular phosphorite at its base and is associated with enigmatic geochemical anomalies (Hsü *et al*. 1985) related to basinwide transgression and euxinic conditions. Marker 'D', which is found in the neighbouring Badaowan Section, marks the FAD of trilobites in South China.

In 1991, the SE Newfoundland section was chosen as the global reference section for the Precambrian–Cambrian boundary (Brasier *et al*. 1994; Landing 1994). Because of the shortcomings of the Newfoundland sections (Brasier *et al*. 1994), global correlation of this Precambrian–Cambrian boundary level can only be carried out using trace-fossil stratigraphy, notoriously difficult in such a condensed and carbonate-rich section as Meishucun. The base of the Cambrian in Newfoundland is defined as the level where the *Harlaniella podolica* assemblage is replaced by an assemblage characterized by *Phycodes pedum*. In siliciclastic sections such as in Newfoundland, characteristic trace fossils usually mark the onset of the Cambrian prior to the appearance of small

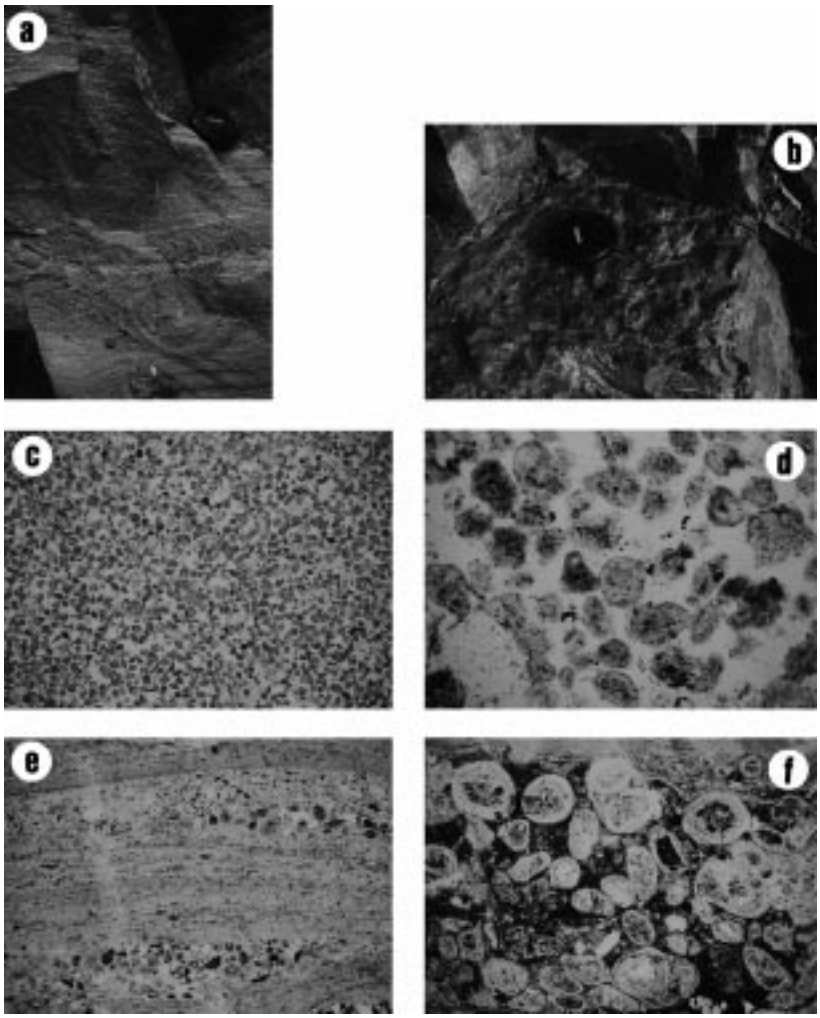

Fig. 4. Field photographs (a, b) and thin-section microphotographs (c, d, e, f) of Meishucun phosphorites: (**a**) Outcrop of clastic phosphorites of unit 6. lens cap is 52 mm; (**b**) outcrop of phosphatized microbial mats of unit 6. Lens cap is 52 mm; (**c**) sample Ix 21, phosphoclastic grainstone, silica cement, photo width is 2.5 mm; (**d**) close-up view of (**c**), photo width is 0.6 mm; (**e**) sample Ix 34, phosphatic bindstone and phosphatized microbial mats, photo width is 2.5 mm; (**f**) close-up view of (e), phosphatic ooids with various nucleii, photo width is 0.6 mm.

shelly fossils (SSFs). However, the first-appearance datum of Cambrian-type trace fossils may occur stratigraphically above that of Cambrian-type SSFs in carbonate-rich sections (Lindsay *et al*. 1996) as is the case in South China. The Meishucun Section was not chosen to be the type-section for the Precambrian–Cambrian boundary owing in part to its condensed nature and thus the possibility of significant hiatuses (Landing 1994), and in part owing to the poor correlation potential of SSFs, many of which appear to be endemic and whose preservation potential is likely to be controlled by '*in-situ*' phosphogenesis (Qian & Bengston 1989; Brasier 1990).

Integrated stratigraphy of the Meishucun Section

At Meishucun, finely laminated dolomites of unit 1 of the Xiaowaitoushan member (Fig. 3) are underlain by a short succession of visibly identical dolomites of the Baiyanshao Member. These are dusty in thin-section with only minor amounts of wispy phosphate. There is no marked lithological change at the Baiyanshao–Xiaowaitoushan boundary and tightly grouped $\delta^{13}C$ values ($-2‰$ to $-1.5‰$) extend through Marker A to the base of the Zhongyicun Member (Brasier *et al*. 1990; Shen *et al*. 1998). The first small shelly fossils are hyolithids of unit 1 and are of the *Anabarites trisulcatus* assemblage (Luo 1980). Qian & Bengston (1989), however, question this low occurrence of shelly fossils at Meishucun and instead place Marker A near the base of unit 3 (Fig. 3). By comparison with Siberia, this assemblage would imply a lower Nemakit-Daldynian affinity (Brasier 1989). The unit 2–3 boundary marks a hardground (Fig. 4b, e, f), which also shows decimetre relief in places and phosphatized stromatolites resting on a scour surface. Units 3 and 4 consist of blue-grey, moderately thick-bedded, intraclastic, granular, 'pseudo-oolitic' and siliceous phosphorite with colour banding (dark phosphorite and light dolomite). Fossil diversity does not change significantly through units 1 to 4 and includes *Anabarites*, *Cambrotubulus, Conotheca* and *Protohertzina* (Xing *et al*. 1991). Unit 5 is commonly found as a pervasively weathered, pale grey, thin-bedded or flaky laminated shale containing abundant pyrite, barite, glauconite and phosphate, and possibly corresponds to a deepening of the basin (Siegmund 1995). Much of this bed can be interpreted as a reworked volcanic tuff based on the presence of volcanic minerals and textural evidence suggesting diagenesis of

volcanic glass. From one location, a single, thin layer of bentonite has been analysed petrographically and isotopically (Compston *et al*. 1992). Their zircon U–Pb ages were recalculated by Sambridge & Compston (1994) yielding a poorly constrained age of *c*. 530 Ma. Unit 6 marks a return to the granular phosphorites of units 3 and 4 showing numerous scour and slide structures indicating a complicated history of reworking (Siegmund & Erdtmann 1995). Their origin as reworked parts of predominantly inner shelf environments is confirmed by the existence of distinct remnants of eroded phosphatic precursor sediments, such as early diagenetically, phosphatized SSFs, oncoids, ooids and hardground fragments. According to Landing (1994), the China B fauna appears above an unconformity at the top of unit 6 marked by a phosphate–quartz pebble conglomerate at both the Meishucun and the Wangjiawan sections in Yunnan Province. Unit 6 belongs to the same shelly fossil zone as units 1 to 4 and contains such micromolluscs as *Hyolithellus* sp. and *Tiksitheca licis*, which are known from the pre-Tommotian of Siberia and Mongolia (Brasier *et al*. 1990, 1996). An abrupt change from thin-bedded tabular phosphorites to more massive cross-bedded phosphorites occurs at the base of unit 7 accompanied by the appearance of a variety of micromolluscs such as *Aldanella, Latouchella* and *Paragloborilus* (Xing *et al*. 1991). Although this assemblage would be typical of the basal Tommotian in Siberia, its appearance in Meishucun does not necessarily herald the end of the Nemakit-Daldynian (Brasier *et al*. 1990), as a significant basal Tommotian unconformity is thought to exist across Siberia (Knoll *et al*. 1995) and a similar assemblage is found in western Mongolia accompanied by pre-Tommotian isotopic signatures (Brasier *et al*. 1996). *Aldanella* and *Latouchella* are also known from levels in Newfoundland regarded as possibly pre-Tommotian by various authors (e.g. Narbonne *et al*. 1987; Landing, 1994).

Trace fossils are unfortunately rare at Meishucun. According to Luo *et al*., (1992), *Phycodes pedum* Seilacher (which marks the base of the Cambrian system in Newfoundland) appears close to the base of unit 6 at Meishucun, which is below China B. However, the scarcity of trace fossils in condensed, carbonate-rich sections such as Meishucun sheds doubt on the use of trace fossils as global markers for the Precambrian–Cambrian boundary. Other early trace fossils such as *Arenicolites* sp. and *Chondrites* sp. occur as low as unit 3 (Xing *et al*. 1991) and these are also found in the Vendian (pre-Tommotian) according to Crimes (1987). Arthropod traces *Rusophycus* and *Cruziana* appear in unit 7 for the first time at China B (Li 1991; Luo *et al*. 1992) while *Monomorphichnus* first appears in unit 6 (Xing *et al*. 1991). Neither *Rusophycus* nor *Cruziana* has been found in Tommotian or Atdabanian beds of Siberia (Jensen *et al*. 1996) and so their presence in unit 7 of Meishucun cannot support the late Tommotian–early Atdabanian assignment for Marker B put forward by Kirschvink *et al*. (1991) and Corsetti & Kaufman (1994). Global correlations based on the poor record of trace fossil appearances in the condensed carbonate-rich sections of Siberia are widely made but have become unacceptable in international stratigraphy. *Rusophycus* and *Cruziana*, however, have both been recorded from below the Bonavista Formation within the thick, trace fossil-rich, siliciclastic sections of Newfoundland. In Newfoundland, *Rusophycus avalensis* first appears within member 2 of the Chapel Island Formation, only 200 m above the first-appearance datum of *Phycodes pedum*, and is generally correlated with a level well below the Tommotian of Siberia (e.g. Narbonne *et al*. 1987; Landing 1994).

Another scour surface can be observed between units 7 and 8. Unit 8 is quite a pure rhombic dolomite with minor phosphate. Pseudomorphs of evaporite minerals and bird's eye structures are suggestive of a shallow water environment with occasional restriction (Siegmund 1995). At the neighbouring Badaowan section, an unconformable surface with large (cm–dm) phosphatic clasts and nodules in a glauconite bearing siltstone overlies unit 8 and begins the Badaowan (Shiyuantou) Member. It is possible that this break is of major significance as it can be traced across South China and India (Brasier 1989), above which are found deeper water black shales of various ages and affinities, based on trilobite assemblages. For example, at Badaowan, trilobites first appear 80 m above Marker C, but they appear immediately above this break near Yichang, Hubei Province (Hsü *et al*. 1985).

In sum, biostratigraphy would tend to suggest that China 'A', the first-appearance datum of small shelly fossils in South China, marks the *Anabarites trisulcatus* zone of the lower Nemakit-Daldynian of Siberia and Mongolia. It has been suggested that Marker 'B' marks the base of the Tommotian in South China (Rozanov 1984). However, the discovery of a significant hiatus at the base of the Tommotian in eastern Siberia puts such correlations on less secure ground (Knoll *et al*. 1995; Brasier *et al*. 1996). Correlations which suggest a Tommotian–Atdabdanian affinity for the whole Meishucun section (e.g. Kirschvink *et al*. 1991; Corsetti & Kaufman 1994) are not supported by biostratigraphy and even the trace fossil markers yield ambiguous information (Jensen *et al*. 1996). Unfortunately, carbon isotope stratigraphy (Brasier *et al*. 1990), magnetostratigraphy (Kirschvink *et al*. 1991) and chronostratigraphy (Compston *et al*. 1992) do not yet add greater resolution than we already possess from biostratigraphy. In the absence of biostratigraphic data to the contrary, we consider that the relevant phosphoritic part of the section, i.e. unit 3 to unit 8 is likely to be of Nemakit-Daldynian affinity, i.e. between *c*. 543 and *c*. 530 Ma, with unit 7 possibly close to the Nemakit-Daldynian–Tommotian boundary in agreement with Brasier *et al*. (1990).

Samples

Geological sampling was carried out on two occasions: in 1991 (Table 1: Meishucun excavation sites A and B, Yunnan Province; Siegmund 1995), and in 1992, by GS (Table 2: Meishucun type section and Laogaoshan sections, Yunnan Province; Maidiping section, Sichuan Province; Tianzhushan section, near Yichang, Hubei Province), Excavation site A and B samples from Meishucun were distinctly less weathered than their equivalents from the Meishucun type section. All samples were analysed petrographically (Siegmund & Erdtmann 1995; Shields 1996) and some relevant aspects of their geochemistry and mineralogy are given in Tables 1 and 2. The three most common and laterally extensive forms of phosphorite are:

(1) granular (pseudo-oolitic), clastic phosphorite swimming in a cherty silica cement yielding 12–24% P_2O_5 in general (Fig. 4a, c, d)—this type occurs in decimetre-scale beds with cross-bedding;
(2) more irregularly granular, peloidal phosphorite (often wispy or partly squashed) with dolomitic cement and some siliciclastic detrital matrix (10–20% P_2O_5)—this type is found as pale/dark alternations of dolomite/phosphorite;
(3) dolomite with small rounded phosphatic peloids and intraclastic rip-up clasts (5–10% P_2O_5).

Other phosphorite samples include stromatolitic, oncolitic hardgrounds (Ix 34; Fig. 4b, e, f; Z 2/3, Z23) and nodular phosphorites

Table 1. *Geochemical and mineralogical data from Lower Cambrian samples collected at Meishucun excavation sites A and B*

Strat. height	Sample	Mineralogical description	$\delta^{34}S$	P_2O_5%	S%	MgO%	Fe_2O_3%	Al_2O_3%	Corg.%	Ce anom.	REE ppm
0.75 m	Ix-3.75	Irreg. gran. phos.; dol. cement; quartz detritus	35.5	16.4	0.12	3.45	0.28	0.41	0.06	0.43	194.2
2.50 m	Ix-2	Irreg. gran. phos.; dol. cement; quartz detritus	33.4	16.4	0.12	3.76	0.40	0.48		0.39	210.3
2.90 m	Ix-1.6	Rounded gran. phos.; dol. cement; quartz detrit.	37.2	ca. <10							
3.20 m	Ix-1.3	Gran. phos. as above with phos. rip up clasts	37.0	ca. <15							
2.45 m	Ix4	Rounded gran. phos.; silica cement	33.0	20.2	0.19	1.64	0.24	0.11	0.13	0.50	204.7
2.60 m	Ix5	Phos. packstone; minor dolomite	33.4	ca. 20							
4.40 m	Ix9	Brown, weathered phos.	32.8	ca. 20							
7.60 m	Ix18	Irreg. gran. phos.; dol. cement; with intraclasts	34.2	18.1	0.13	2.86	0.33	1.99	0.07	0.76	370.3
8.25 m	Ix20	Irreg. gran. phos.; dol. cement; with intraclasts	34.1	16	0.10	5.08	0.34	0.29	0.07		
8.50 m	Ix21	Rounded granular phosphorite; silica cement	32.4	11.9	0.08	1.25	0.30	0.21	0.07	0.57	199.8
8.65 m	Ix22	Rounded granular phosphorite; silica cement	31.7	ca. 12							
9.20 m	Ix23	Rounded granular phosphorite; silica cement	32.3	24.1	0.18	1.64	0.24	0.27	0.15	0.42	164.5
9.60 m	Ix24	Rounded granular phosphorite; silica cement	33.2	ca. <15							
10.1 m	Ix25	Phosphatic chert; Fe oxides; 40% silica	34.3	6.9	0.04	11.52	1.14	0.70	0.09	0.30	73.4
10.4 m	Ix26	Rounded gran. phos.; dol. cement; quartz detr.	33.6	ca. 15							
11.5 m	Ix28	Dolomite with irregular phosphatic clasts	34.5	10	0.06	8.95	0.44	0.43	0.02	0.30	99.1
12.4 m	Ix29	Dolomite with irregular phosphatic clasts	34.2	ca. <10							
12.5 m	Ix30	Dolomite with red, rounded, phosphatic clasts	32.2	ca. <10							
13.0 m	Ix31	Dolomite with red, rounded, phosphatic clasts	25.3	ca. <10							
13.8 m	Ix33	Irreg. gran. phos.; dol. cement; quartz detr.	31.4	ca. 15							
14.0 m	Ix34	Brown phosphatic stromatolite, detritus	31.5	21.1	0.13	1.97	1.64	0.97	0.2	0.72	265.5
14.1 m	Ix35	Dolomitic, phosphatic sandst.; ca. 40% quartz	31.8	11.9	0.06	4.98	1.06	2.64	0.09	0.69	458.3
16.7 m	Ix40	Brown, phosphoritic basal conglomerate; chert	31.8	14.7	0.09	1.87	2.91	5.70	0.07	0.80	709.7

Further information may be found in Siegmund (1995) and Siegmund & Erdtmann (1995). *c.* P_2O_5 data represent estimated phosphate concentrations made by comparing measured data from 12 samples and thin-sections. Ce anomaly = $3Ce_{ASC}/(2La_{ASC}+Nd_{ASC})$ (Altschuler 1980). REE data are for the 2 N HCl soluble fraction, whereas other elemental contents are bulk rock XRF data.

Table 2. *Sulphur isotope data and mineralogical information for several lower Cambrian phosphorites from South China*

Strat. height	Sample name	Location	Mineralogical description	$\delta^{34}S$
0.1 m	Z2/3b	Unit 3, Meishucun, Yunnan province	Granular phosph. hardground, dolomite cement	33.1
0.1 m	Z2/3b	Unit 3, Meishucun, Yunnan province	Granular phosph. hardground, dolomite cement	32.6
0.2 m	Z23	Unit 3, Meishucun, Yunnan province	Granular phosph. hardground, dolomite cement	33.6
0.5 m	Z>2/3	Unit 3, Meishucun, Yunnan province	Phosphatic dolomite	17.4
1.7 m	Z25	Unit 3, Meishucun, Yunnan province	Irreg. and rounded phos.; dol. cement; detritus	32.1
2.5 m	Z43	Unit 3, Meishucun, Yunnan province	Dolomitic phosphorite	31.6
3.3 m	Z26	Unit 4, Meishucun, Yunnan province	Rounded gran. phos.; silica cement	31.1
8.6 m	Z27	Unit 6, Meishucun, Yunnan province	Irreg. phosphatic dolomite; quartz detritus	30.1
9.5 m	Z38a	Unit 6, Meishucun, Yunnan province	Brown, rounded gran. phos.; silica cement	29.7
9.5 m	Z38b	Unit 6, Meishucun, Yunnan province	Brown, rounded gran. phos.; silica cement	30.9
13.5 m	Z39	Unit 7, Meishucun, Yunnan province	Phosphatic dolomite; quartz crystals	29.0
9.5 m	L2	Unit 6, Laogaoshan, Yunnan province	Blue weathered, fossilif. phosph.; silica cement	33.1
—	T10	Tianzhushan, Hubei province	Centimetre-thick phosphorite bands in dolomite	33.2
—	M20	Unit 31e/32, Maidiping, Sichuan province	Brown, gran. phosphorite/dolomite alternations	30.2
—	M21	Unit 32, Maidiping, Sichuan province	Phosphorite/dolomite alternations	31.7
—	M11	Unit 34/35, Maidiping, Sichuan province	Phosphorite/dolomite alternations	30.5
—	M13	Unit 35, Maidiping, Sichuan province	Phosphorite/dolomite alternations	31.2

Units for Meishucun data are shown in Fig. 3. Palaeontological data (Brasier *et al.* 1990) shows that Sichuan and Hubei Province samples are of ages similar to those of Meishucun.

(Ix 40). Petrographic and geochemical analyses demonstrated that all phosphorite samples (units 3, 4, 6, 7) contained some detritus and were pyrite and organic carbon-poor. However, units 5 and 9 of Meishucun are richer in pyrite and relatively poor in phosphorite (<5% P_2O_5).

Phosphate-bound sulphate

As discussed above, in order to constrain seawater $\delta^{34}S$ with more confidence, it is becoming necessary to analyse trace sulphate in marine authigenic minerals such as carbonate and phosphate, which are generally more abundant and more likely than evaporite minerals to incorporate an open ocean signal (Strauss 1996). Biogenic carbonate has already been used successfully for this purpose for the Neogene (Burdett 1989) and for the Mesozoic and Palaeozoic (Kampschulte & Strauss 1996, 1998).

Sulphate is present in unaltered phosphorites at up to 2.7 wt% with the amount of substitution depending on the concentration of SO_4^{2-} in the aqueous phase in equilibrium with francolite (Jarvis *et al.* 1994). Sulphate is substituted into the phosphate lattice with little fractionation from seawater $\delta^{34}S$ similar to that for evaporitic sulphate minerals, i.e., about +1.5‰ (Smirnov *et al.* 1962; McArthur *et al.* 1986).

Some 21 sulphur isotope measurements obtained from sulphate within sedimentary carbonate fluorapatite from phosphorite deposits, first demonstrated that $\delta^{34}S$ values from phosphorites often match the range of values reported from coeval evaporites (Bliskovskiy *et al.* 1977). For example, as part of this pioneering study, two Lower Cambrian phosphates from Aksay and Dzhanatas on the Siberian Platform yielded $\delta^{34}S$ values of 32.1‰ and 31.9‰ (CDT), respectively, practically identical to those of coeval evaporites from the Siberian Platform already discussed (Fig. 1; Pisarchik & Golubchina 1975; Claypool *et al.* 1980). However, phosphate samples from the Permian and Eocene were exceptions and displayed anomalously high $\delta^{34}S$ values. As is the case for sedimentary barite (Cecile *et al.* 1983), phosphorite can unfortunately yield $\delta^{34}S$ values both higher and lower than coeval evaporite successions (Benmore *et al.,* 1983; Jarvis *et al.* 1994) leading to significant ambiguity of interpretation. In order for this approach to be fruitful, therefore, it is necessary to select samples which are most likely to yield seawater S isotope signatures. The interpretation of $\delta^{34}S$ values from phosphate-bound sulphate is not straightforward because redox conditions of formation and diagenesis must also be taken into account. Recent studies have concluded that sulphate bound up in the phosphate lattice may have undergone significant isotopic fractionation with respect to seawater, (e.g. McArthur *et al.* 1986; Jarvis *et al.* 1994; Poulton *et al.,* 1998) depending on redox conditions during phosphate genesis and pyrite formation. Where phosphate precipitates or undergoes early diagenesis in a closed or semi-closed system in which pyrite is forming, the large fractionation involved in the reduction of sulphate to sulphide will serve to preferentially remove lighter sulphur from the system causing $\delta^{34}S/^{32}S$ to increase in ambient fluids. Alternatively, the reoxidation of this pyrite can cause isotopically light sulphur to be released causing $\delta^{34}S$ to decrease in ambient waters at the boundary between sulphate reducing and oxic conditions (Benmore *et al.* 1983). In general, phosphate that forms and/or undergoes diagenesis in oxic or suboxic realms may retain a seawater $\delta^{34}S$ signature but phosphate which was formed in parts influenced by sulphate reduction in the anoxic parts of the sediment column is likely to yield $\delta^{34}S$ values higher than coeval seawater. McArthur & Walsh (1984) proposed that Ce anomalies might help to indicate whether significant isotopic fractionation of seawater $\delta^{34}S$ has taken place. For example, significant Ce depletion (i.e., negative Ce anomalies) could be taken to imply oxic conditions of deposition and diagenesis, whereas no light REE fractionation could be taken to imply anoxic or suboxic reequilibration of redox sensitive species, and therefore, likely isotopic fractionation due to pyrite formation. In a later paper, however, McArthur *et al.* (1986) rejected the notion that either phosphate morphology and/or the presence/absence of Ce anomalies could serve as guides to likely sulphur isotopic fractionation during the genesis of sedimentary phosphate. Although phosphate Ce anomalies can indeed lend themselves to ambiguous interpretation (Holser 1997), phosphorite morphology may be a crucial criterion in determining conditions of deposition and diagenesis, and along with other criteria, such

as the presence of pyrite or organic carbon, can help us establish whether the immediate environment was likely to have been influenced by sulphate reduction (e.g. Poulton *et al*., 1998). The rounded clastic nature of the mostly granular S China phosphorites implies that the sediments experienced extensive and repeated reworking close to the sediment–water interface, while the pale colour and general lack of pyrite and organic matter imply that early diagenesis was not significantly influenced by sulphate reduction. Ilyin (1998) reaches a similar conclusion while attempting to explain the preservation of seawater-type REE patterns and Ce anomalies in ancient granular phosphorites, including several from the Meishucun Section. We argue that cerium ought to react more sensitively to lowering oxidation potential than sulphate, with redistribution of the REE and cerium (III) in the sediment even under suboxic conditions (German & Elderfield 1990; Holser 1997). Therefore, the preservation of a significant, seawater-like Ce anomaly in phosphorites, lower than about 0.4 (Table 1), can be expected to indicate an early diagenetic environment relatively unaffected by microbially mediated redox recycling and sulphate reduction. However, the absence of a significant Ce anomaly would lead to more ambiguous interpretation (McArthur *et al*., 1986).

Timing of phosphogenesis

Constraining the timing of phosphogenesis is of crucial importance to determining whether non-seawater influences are likely to be detectable on the sulphate sulphur isotope ratio. Siegmund & Erdtmann (1995) found evidence for direct precipitation of apatite in the form of isopachous or spherulitic hexagonal apatite crystals in microbial mats and nodules and suspected microbial mediation throughout South China. However, at Meishucun, all the phosphorite except for rare examples of phosphatized stromatolites and nodules are interpreted to be reworked phosphatic mudstones with little '*in-situ*' phosphogenesis after deposition in a demonstrably oxic environment (extensive bioturbation in all units except 5 and 9). The rounded nature of the grains derives from their exposure to a high-energy seawater environment and reworking close to the sediment–water interface, whereas their presently, uncompacted nature and early cementation (Fig. 4) indicates an early closing of the diagenetic system to further alteration and sulphate reduction at depth. This redeposition in a dynamic environment where little sulphate reduction or organic carbon burial can be established would be favourable to retaining initial sulphate sulphur isotope ratios. It is therefore argued that the Chinese granular phosphorite samples from units 3, 4, 6 and 7 at Meishucun are likely to yield $\delta^{34}S$ values close to those of coeval seawater.

Analytical methods

All samples were crushed, picked and ground into a fine powder, which was then washed thoroughly in distilled water. Only the samples listed in Table 1 were subsequently washed in a dilute NaCl solution (Kampschulte & Strauss 1998), in order to remove easily soluble sulphates, during which the supernate of these cleaning steps was allowed to react with $BaCl_2$ until no white precipitate could be detected. In this study, sample leaching was not carried out under an inert atmosphere, such as nitrogen or argon (Louie *et al*. 1995; Poulton *et al*. 1998), something which is certainly to be recommended for all future studies. The omission of an inert atmosphere can be justified in our study as no phosphorite-rich samples yielded any white precipitate during washing, which underlines the low potential for the incorporation of sulphate from sulphide oxidation in the sample analyses. The resultant solution was centrifuged and filtered through Micropore® filters. A saturated solution of $BaCl_2$ was added and any sulphate ions present were immediately precipitated as $BaSO_4$. After about ten minutes, this liquid was filtered and the residue dried, ready for combustion. Repeated measurements of single samples show that this preparation technique resulted in isotopically homogeneous powders. XRD analyses resolved only the presence of barite. Sulphur dioxide for sulphur isotopic analyses was prepared by combusting the barium sulphate using standard techniques (Coleman & Moore 1978; Yanagisawa & Sakai 1983) at ETH Zürich, Switzerland, at the University of Vermont, USA (Table 2) and at the Ruhr-Universität, Bochum, Germany (Table 1). ETH data are not reported here as only replicate analyses were made as a check. Liberated SO_2 was cryogenically packed into 6 mm pyrex tubes. Isotopic analyses were made on VG 903, SIRA II and Finnegan MAT 251 mass spectrometers, respectively. Working gases were calibrated against internationally recognised standards. Reproducibility, as determined through replicate analyses, was generally better than 0.3‰. Sulphur isotopic compositions are expressed as per mil deviations ($\delta^{34}S$) from Canyon Diablo Troilite (CDT). Bulk sulphur, magnesium, iron, aluminium, phosphorus and carbon contents were measured using X-ray fluorescence and calcination techniques (Siegmund 1995). REE contents were measured using ICP-MS at the CGS Strasbourg on HCl-soluble leachates (Shields 1996). Ce anomalies are reported normalized to shale (NASC of Altschuler 1980).

Results

Table 1: excavation sites A and B (Kunyang Mine)

The $\delta^{34}S$ data are tightly grouped ranging between 31‰ and 37‰ (Fig. 5) with one phosphate-poor outlier (Ix 31 = 25.3‰). There appears to be no simple relationship between $\delta^{34}S$ and either phosphate, sulphur, organic carbon, iron or dolomite contents or Corg/S ratios (Fig. 6). However, with the exception of Ix 18, there does appear to be a certain correlation between seawater-type low Ce anomalies and high $\delta^{34}S$ values. Figure 7 shows S content to be linearly correlated with P_2O_5 content in these samples. The slope and intercept of the covariation imply that the Meishucun phosphorites contain a maximum of only 0.6% SO_4, with sulphate ions replacing approximately 2% of phosphate ions in the apatite lattice, and confirm that there is negligible pyrite-derived sulphur. For comparison, unweathered Cenozoic francolites contain *c*. 32% P_2O_5, 52% CaO, 4% F and $2.7 \pm 0.3\%$ SO_4 (Jarvis *et al*. 1994).

Table 2: Meishucun type section (Kunyang Mine)

$\delta^{34}S$ data from the more weathered samples of the Meishucun type section (Table 2) are also tightly grouped with values between 29‰ and 33‰. Comparison with Table 1 data (Fig. 5) shows that values from Meishucun type-section are generally lower than those from excavation sites A and B. Phosphorite samples from the correlative Maidiping section in Sichuan Province (M11, M13, M20 and M21) yield similar $\delta^{34}S$ values between 30.2 and 31.7‰. These samples can be placed stratigraphically between Markers A and B, i.e. within units 3 to 6 (following Brasier *et al*. 1990). One sample from the similarly condensed Tianzhushan section in Hubei Province (T10) is also placed between markers A and B and yielded a value of 33.2‰.

Discussion

The absence of evidence for local pyritization, the distinctly early cementation (Fig. 4), the history of reworking in oxic,

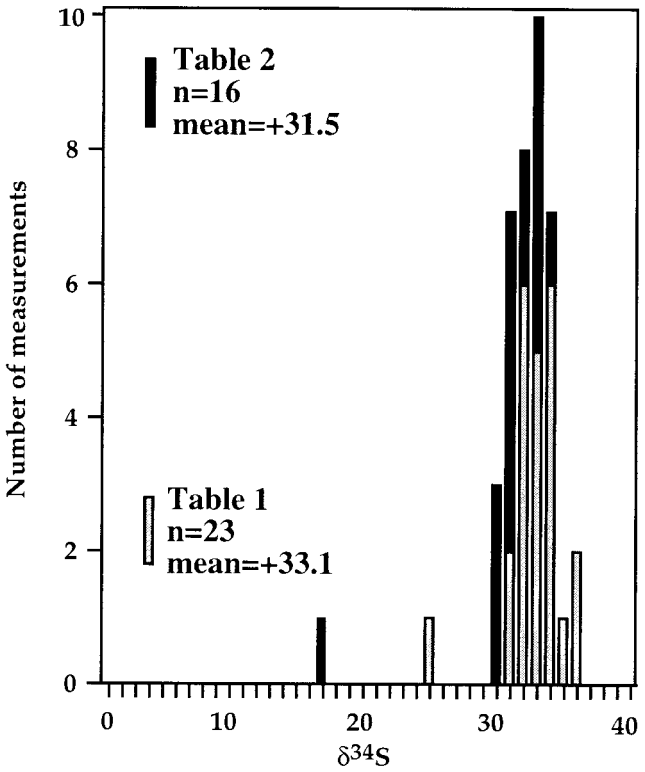

Fig. 5. Histogram of $\delta^{34}S$ data values for Meishucun section and correlatives shows most values between 31‰ and 35‰. For Table 2 samples, one the outliers visible in the figure have not been used to calculate the mean. The mean $\delta^{34}S$ of all phosphorites (>50% francolite)=32.8‰ (n=35).

marine waters, the preservation of seawater-like Ce anomalies, and consistency with other evaporite-based data for the Vendian–Cambrian lead independently to the conclusion that the high $\delta^{34}S$ values of the Meishucun phosphorites and correlatives faithfully record the seawater sulphur isotopic composition at the time of phosphogenesis and early diagenesis, i.e. *c*. 33‰ (± 4‰), bearing in mind that there will have been some fractionation from seawater of about +1.5‰ (Jarvis *et al*. 1994). Low outliers such as Ix 31 and Z >2/3 (Fig. 5) are consistent with the inadvertent incorporation of sulphate derived from pyrite oxidation, either during diagenesis or sample preparation.

The phosphorite $\delta^{34}S$ values from South China are similar to those obtained from Lower Cambrian barites from South China (Wang & Li 1991), which lie between 31 and 40‰ (mean=35‰; n=20), implying that those barite deposits also formed in an environment dominated by seawater sulphate. However, both these and our data differ from those obtained by Shen *et al*. (1998) for five phosphate-bound sulphate analyses of Meishucun phosphorite (mean=24.2‰) and two samples of stratigraphically higher phosphorite concretions (mean=36.9‰). These data were interpreted to reflect a rise in seawater $\delta^{34}S$ of 12.7‰ for the 'terminal Proterozoic to the early Cambrian' (Shen *et al*. 1998). As mentioned above, there is no biostratigraphic evidence that the Meishucun Section contains phosphorite of Terminal Proterozoic age. In the absence of any detailed description of the preparation of these samples, or their precise stratigraphic positions, it is difficult to compare these data with the data herein. However, our results show no evidence of such a change, implying that the rise to high $\delta^{34}S$ must have occurred earlier than the deposition of unit 3 of the Meishucun Section. It should also be pointed out that the highly reducing nature of the sediments and concretions overlying the Meishucunian phosphorites throughout South China would not have been an appropriate diagenetic environment for the preservation of a seawater $\delta^{34}S$ signature (McArthur *et al*. 1986; Jarvis *et al*. 1994) as is maintained by Shen *et al*. (1998).

Meishucun data in this paper show decreasing $\delta^{34}S$ up section: 33–29‰ and *c*. 35–37‰ to 31.5‰ for the type section, and Meishucun A and B, respectively. Both absolute values and a subtle trend to lower values are consistent with Siberian data (Claypool *et al*. 1980), for which a long term trend could be identified from *c*.>33‰ to *c*. 29‰ in Vendian–lower Middle Cambrian evaporites. According to the correlation we are following, i.e. that the Meishucun section is predominantly Nemakit-Daldynian in age, the samples herein would fit into the uppermost Vendian–Cambrian part of the Claypool *et al*. (1980) data from Siberian evaporites (Fig. 1). The implication from the Claypool *et al*. data is that Vendian–Cambrian boundary seawater $\delta^{34}S$ is likely to have been at least as high as 32‰, something which our study supports with a mean $\delta^{34}S$ value of 32.8‰ (n=35) (Fig. 5).

Absolute values from the Meishucun type-section are consistently offset lower by an average of 2‰ from the data of excavation sites A and B at Kunyang mine (Fig. 5). Conscientious measuring of internationally recognized standards by both laboratories rules out significant interlaboratory bias. The more weathered state of the Meishucun type-section samples may have resulted in the incorporation of pyrite derived sulphate in the analyses of these samples leading to a slight lowering of the measured $\delta^{34}S$. However, the equally low values (30–31‰) from the pyrite-poor samples of Maidiping in Sichuan Province argue against this. It is perhaps more likely that differences between these neighbouring sections reflect primary differences in the depositional and diagenetic environments. In either case, it is advisable not to regard any particular value as most representative of early Cambrian seawater at this stage and instead rely on the mean value as the best approximation, i.e. 32‰ (± 2‰), (1.5‰ needs to be subtracted to account for fractionation during incorpoaration of seawater sulphate ions into phosphate). In this regard, it may be important to note that samples which have retained the most pronounced Ce anomalies characteristic of open seawater (Table 1: Samples Ix − 3.75, Ix − 2, Ix 23, Ix 25, Ix 28) yield a high average of 34.0‰ (Fig. 6).

It is more difficult to interpret the short-term stratigraphic variations in $\delta^{34}S$ within our more complete data set (Fig. 3). The ocean residence time of SO_4^{2-}, is about 12 Ma (Jarvis *et al*. 1994) and as such is much longer than the present day ocean mixing time of about 2000 years (Holland 1984). This means that seawater $^{34}S/^{32}S$ ratio should be the same worldwide at any one time and any changes are likely to be sluggish, even on a geological time scale. Therefore, it is difficult to imagine that, for example, the drop to lower values close to the base of unit 6 can reflect changing sulphur isotopic ratio in the oceans. These variations are more likely due to variations in the openness of the basin or in the early diagenetic environment.

High seawater $\delta^{34}S$ and biogeochemical cycling

Data herein, and other data already published for the Cambrian, help to constrain the rise in seawater $\delta^{34}S$ to prior

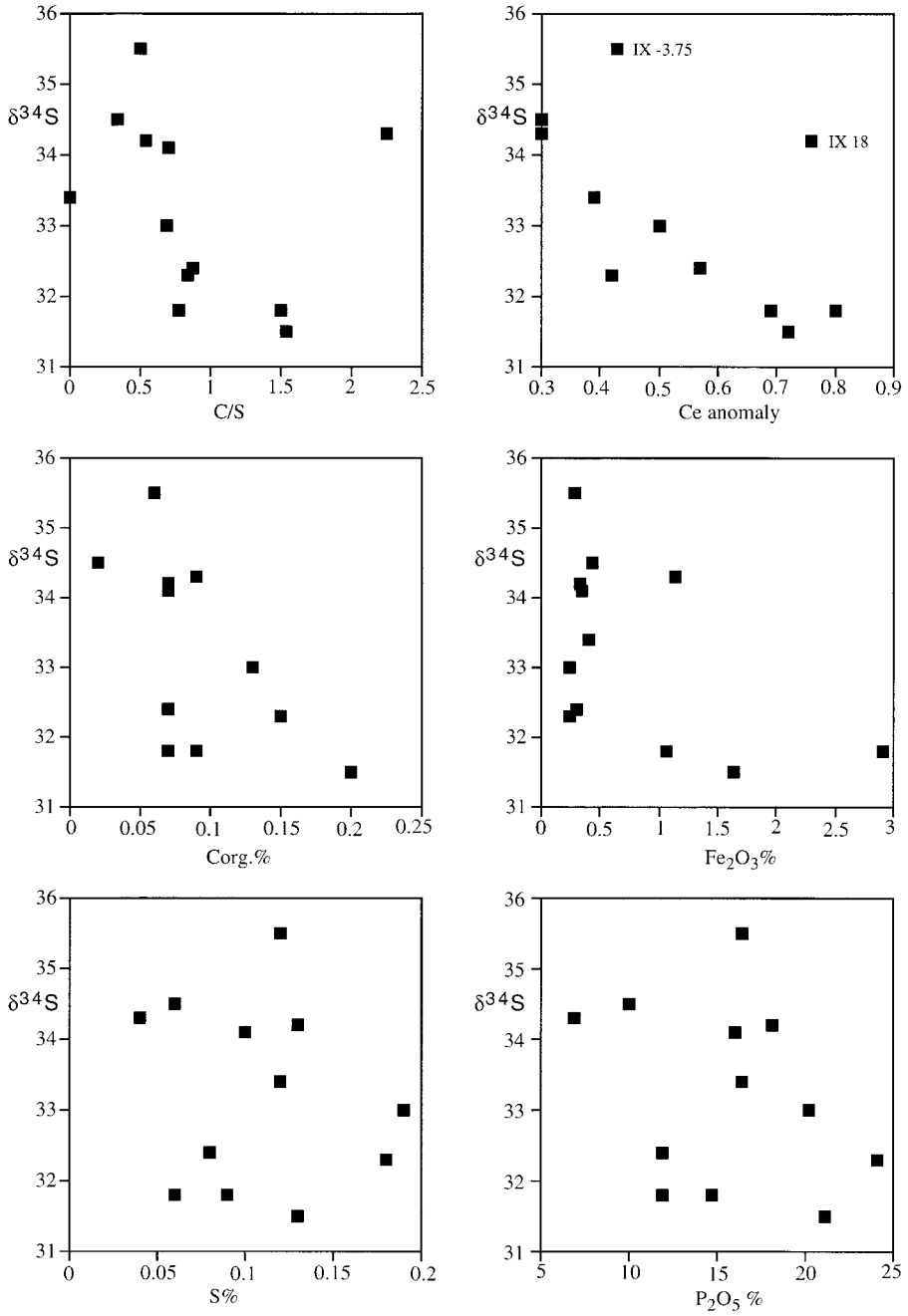

Fig. 6. Cross plots of several geochemical parameters (Corg/S ratio, Ce anomaly and percentage Corg., Fe, S and phosphate contents) against sulphate $\delta^{34}S$.

to the Cambrian, and conflict with the views of Shen *et al.* (1998). Neoproterozoic data are, however, currently insufficient to constrain the timing of this rise with more precision. Nevertheless, high $\delta^{34}S$ values of between 25 and 32‰ from Neoproterozoic evaporites in Brazil (Misi & Kyle 1994; Misi & Veizer 1998) and the continuation of high $\delta^{34}S$ through the Cambrian (Fig. 1) now make it difficult to maintain the existence of a catastrophic and geologically instantaneous rise in seawater $\delta^{34}S$ close to the Precambrian–Cambrian boundary as proposed by Holser (1977), and thereby remove any similarity with $\delta^{34}S$ events in the mid-Devonian and Early Triassic periods.

What were the reasons for such high $\delta^{34}S$ in seawater? Several authors have considered that high $\delta^{34}S$ existed at the same time as high $\delta^{13}C$ (up to +11‰) in the late Neoproterozoic oceans (e.g. Derry *et al.* 1992). Thus, the high levels of organic matter burial, implicit from the carbon isotope record for this time, would not appear to have been balanced by sulphate reduction, thereby allowing photosynthetically produced oxygen to build up in the atmosphere (Derry *et al.* 1992; Shields *et al.* 1997). However, it is still unclear whether anomalously high $\delta^{34}S$ did exist at the same time in the oceans as high $\delta^{13}C$ owing to poor stratigraphical resolution. We consider it more likely that seawater $\delta^{13}C$ and $\delta^{34}S$ were *negatively* coupled in the latest Proterozoic with the rise in $\delta^{34}S$ paralleling a long-term decrease in $\delta^{13}C$. In addition, it also appears likely that at least part of this rise in seawater $\delta^{34}S$ was caused by other mechanisms.

Canfield & Teske (1996) put forward new evidence for a significant increase in the biologically controlled isotopic

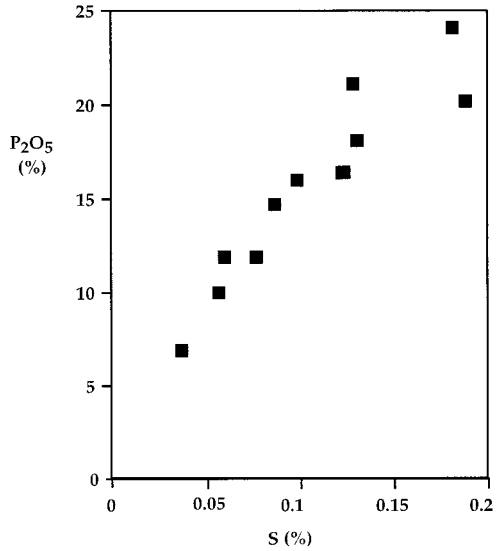

Fig. 7. Whole rock XRF data showing generally linear correlation between phosphate and sulphur contents (linear regression equation = $113.5y + 3.1x$, with $r^2 = 0.90$). Only minor amounts of pyrite in the samples suggest that most of the sulphur is bound up in the francolite lattice, replacing up to 2% of the phosphate, as opposed to up to 8% in recent francolites (Jarvis *et al.* 1994).

discrimination between the sulphate and sulphide reservoirs sometime between 1.05 and 0.64 Ga. This increase, they maintain, was related to the evolution of non-photosynthetic, sulphide-oxidizing bacteria around this time. They argue that this evolutionary event was related to the appearance of a suboxic layer within the Precambrian water column, where these biologically mediated reduction and oxidation processes could take place. The consequence of both sulphide oxidizing and sulphate reducing bacteria working within the water column at this time would have been to increase the range of $\delta^{34}S$ values in pyrite and might help in part to explain the rise to high $\delta^{34}S$ values during the latter part of the Neoproterozoic without invoking greater amounts of sulphate reduction. An additional and related factor is the introduction of macrobioturbation, which is likely to have commenced sometime after 600 Ma (Brasier & McIlroy 1998). It is well known that, for oxygen-poor sediments, bioturbation may play an inordinately significant role in the redistribution of organic matter while at the same time increasing fluxes of seawater derived oxygen (Aller 1978) and sulphate (Bloch & Kruse 1992) to this organic matter. One effect of macrobioturbation today on the sulphur cycle is to create the conditions necessary for the reoxidation of diagenetic sulphide (Fisher 1986). Sulphide oxidation itself is rapid and does not involve any significant isotopic fractionation (Nakai & Jensen 1964). Therefore, resultant sulphate will have the same $\delta^{34}S$ values as the precursor pyrite and will be depleted in ^{32}S relative to seawater, by up to 46‰ (Chambers & Trudinger 1979). Further reduction of this reintroduced sulphate will lead to sulphides extremely depleted in ^{34}S. This phenomenon of sulphide reoxidation is frequently invoked to explain the large natural variation in sulphide sulphur isotopic compositions, which show $\delta^{34}S$ values up to 70‰ more depleted than coeval seawater (e.g. Fisher 1986; Canfield & Teske 1996; Poulton *et al.* 1998). Therefore, the introduction of penetrative bioturbation would have also served to increase isotopic fractionation during the formation of pyrite in early diagenesis, thus helping to increase seawater $\delta^{34}S$ values without the necessity for greater amounts of sulphate reduction.

An additional factor which must be considered is the appearance of metazoans themselves on the surface of the Earth sometime in the late Neoproterozoic, and their flourishing close to the beginning of the Cambrian, *c.* 543 Ma. This aspect, although clearly of importance for biogeochemical cycling, has not enjoyed the attention it deserves. The effect of metazoan activity before the Cambrian explosion, e.g. the introduction of faecal pellets (Logan *et al.* 1995), and the activity of suspension feeders such as sponges (Brasier *et al.* 1997), would have served to gradually lower the redox boundary from within the water column to the seafloor (Logan *et al.* 1995; Shields *et al.* 1999), and hence the activities of sulphur-utilizing bacteria would have eventually become restricted to a position close to the sediment–water interface, much as today. Metazoans would have initially enhanced organic matter burial due to bottom water anoxia (Logan *et al.* 1995), hence the extremely high $\delta^{13}C$ values in late Neoproterozoic oceans (e.g. Derry *et al.* 1992; Brasier *et al.* 1996). However, the subsequent introduction of macrobioturbation (Brasier & McIlroy 1998) and filter feeding would have increased the efficiency of organic matter recycling. As we have seen, sulphide reduction came to be associated with greater isotopic discriminations due to bioturbation related sulphide reoxidation. However, oxic organic decay (Brasier & McIlroy 1998) and associated sulphate reduction (Fisher 1986) would also have become more efficient due to enhanced oxygen and sulphate redistribution through bioturbation. Therefore, the distinct Neoproterozoic–Cambrian isotopic trends to high $\delta^{34}S$ (from 15‰ to 33‰) and to low $\delta^{13}C$ (from +11‰ to −4‰) may also be explained by a biogenically catalysed increase in organic carbon reoxidation–respiration coupled with an increase in sulphate reduction.

Conclusions

Phosphate-bound sulphate can faithfully incorporate the S-isotopic composition of ambient seawater with minor fractionation. From a comparison of our data with those in the literature, we conclude that 32‰ (±2‰) is a reasonable minimum estimate for seawater sulphate $\delta^{34}S$ during the earliest Cambrian or Nemakit-Daldynian (*c.* 540 Ma) and that $\delta^{34}S$ is likely to have fallen during the subsequent parts of the early Cambrian to *c.* 28‰ by the mid-Cambrian. Present data for the upper Neoproterozoic are scarce. Nevertheless, they are consistent with a rise from a plateau of low values (<20‰) sometime after 750 Ma to the Precambrian–Cambrian boundary. Part of the rise can be explained by a change in the isotopic discrimination between sulphate and sulphide in the oceans brought on by the actions of sulphur-oxidizing bacteria, particularly after the introduction of penetrative bioturbation close to the Neoproterozoic–Cambrian transition, whereas some part may relate to the lowering of the redox boundary in seawater and consequent increases in the efficiency of organic matter degradation and sulphate reduction at this time. We consider that by constraining the beginning of the rise in seawater $\delta^{34}S$ sometime in the late Neoproterozoic we may help to pinpoint biological events such as the introduction of bioturbation and the evolution of particular types of metazoans and their effects on global biogeochemical cycling. Further constraints on sulphur isotope stratigraphy at this time await future studies on trace sulphate in marine authigenic minerals.

The authors would like to thank sincerely M. Brasier, S. Bottrell, I. Fairchild, Y. Jiedong, P. Stille, S. Bernasconi and O. Kuhn for their helpful insights and critical reviews during various stages of this project. The senior author gratefully acknowledges the financial support of the National Science Foundation of Switzerland and the Academie des Sciences of France (Société de Secours des Amis des Sciences). The helpful assistance of the Chinese Academy of Sciences, and especially Xiao Wenjiao and Zhang Shishen are gratefully acknowledged. This is a contribution to IGCP Project 386: Response of the ocean/atmosphere system to past global changes.

References

Aller, R.C. 1978. The effect of animal-sediment interactions on geochemical processes near the sediment-water interface. *In*: Wiley, M.L. (ed.) *Estuarine interactions*. Academic Press, New York, 157–172.

Altschuler, Z.S. 1980. The geochemistry of trace elements in marine phosphorites Part 1. Characteristic abundances and enrichment. *In*: Bentor, Y.K. (ed.) *Marine phosphorites; geochemistry, occurrence, genesis. SEPM Special Publication*, **29,** 19–30.

Benmore, R.A., Coleman, M.L. & McArthur, J.M. 1983. Origin of sedimentary francolite from its sulphur and carbon isotope composition. *Nature,* **302,** 516–518.

Bliskovskiy, V.Z., Grinenko, V.A., Migidisov, A.A., Savina, L.I. & Vernadskiy, V.I. 1977. Sulphur isotopic compositon of the minerals of phosphorites. *Geochemistry International,* **8,** 148–153.

Bloch, J. & Krouse, H.R. 1992. Sulfide diagenesis and sedimentation in the Albian Harmon Member, western Canada. *Journal of Sedimentary Petrology,* **62,** 235–249.

Brasier, M.D. 1989. China and the Palaeotethyan Belt (India, Pakistan, Iran, Kazakhstan, and Mongolia). *In*: Cowie, J.W. & Brasier, M.D. (eds) *The Precambrian–Cambrian boundary*. Clarendon Press, Oxford, 117–165.

—— 1990. Phosphogenic events and skeletal preservation across the Precambrian–Cambrian boundary interval. *In*: Notholt, A.J.G. & Jarvis, I. (eds) *Phosphorite Research and Development*. Geological Society, London, Special Publications, **52,** 289–303.

—— & McIlroy, D. J. 1998. Neonereites uniserialis from *c.* 600 Ma year old rocks in western Scotland and the emergence of animals. *Journal of the Geological Society of London,* **155,** 5–12.

——, Cowie, J. & Taylor, M. 1994. Decision on the Precambrian-Cambrian boundary stratotype. *Episodes,* **17,** 1 & 2, 3–8.

——, Green, O. & Shields, G.A. 1997. Ediacarian sponge spicules from western Mongolia and the origins of the Cambrian fauna. *Geology,* **25,** 303–306.

——, Margaritz, M., Corfield, R., Luo, H., Wu, X., Ouyang, L., Jiang, Z., Hamdi, B., He, T. & Fraser, A.G. 1990. The carbon and oxygen isotope record of the Precambrian-Cambrian boundary interval in China and Iran and their correlation. *Geological Magazine,* **127,** 4, 319–332.

——, Shields, G.A., Kuleshov, V.N. & Zhegallo, E.A. 1996. Integrated chemo- and biostratigraphic calibration of early animal evolution: Neoproterozoic-early Cambrian of southwest Mongolia. *Geological Magazine,* **133,** 4, 445–485.

Burdett, J.W., Arthur, M.A. & Richardson, M. 1989. A Neogene seawater sulphur isotope curve from calcareous pelagic microfossils. *Earth and Planetary Science Letters,* **94,** 189–198.

Canfield, D.E. & Teske, A. 1996. Late Proterozoic rise in atmospheric oxygen concentration inferred from phylogenetic and sulphur-isotope studies. *Nature,* **382,** 127–132.

Cecile, M.P., Shakur, M.A. & Krouse, H.R. 1983. The isotopic composition of western Canada barites and the possible derivation of oceanic sulphate $\delta^{34}S$ and $\delta^{18}O$ age curves. *Canadian Journal of Earth Sciences,* **20,** 1528–1535.

Chambers, L.A. & Trudinger, P.A. 1979. Microbiological fractionation of stable sulfur isotopes. *Geomicrobiology Journal,* **1,** 249–292.

Claypool, G.E., Holser, W.T., Kaplan, I.R., Sakai, H. & Zak, I. 1980. The age curves of sulphur and oxygen isotopes in marine sulphate and their mutual interpretation. *Chemical Geology,* **28,** 199–260.

Coleman, M.L. & Moore, M.P. 1978. Direct reduction of sulfates to sulfur dioxide for isotopic analysis. *Analytical Chemistry,* **50,** 1594–1595.

Compston, W., Williams, I.S., Kirschvink, J.L., Zhang, Z. & Ma, G. 1992. Zircon U-Pb ages for the Early Cambrian time-scale. *Journal of the Geological Society, London,* **149,** 171–184.

Cook, P.J. & Shergold, J.H. (eds) 1986. *Proterozoic and Cambrian phosphorites*. Phosphate deposits of the World, **1,** Cambridge University Press, Cambridge.

Corsetti, F.A. & Kaufman, A.J. 1994. Chemostratigraphy of Neoproterozoic units, White-Inyo Region, Eastern California and Western Nevada: Implications for global correlation and faunal distribution. *Palaios,* **9,** 211–219.

Cowie, J.W. 1985. Continuing work on the Precambrian-Cambrian boundary. *Episodes,* **8,** 93–97.

Crimes, T.P. 1987. Trace fossils and correlation of Late Precambrian and Early Cambrian strata. *Geological Magazine,* **124,** 97–119.

Derry, L.A., Kaufman, A.J. & Jacobsen, S.B. 1992. Sedimentary cycling and environmental change in the Late Proterozoic: evidence from stable and radiogenic isotopes. *Geochimica et Cosmochimica Acta,* **56,** 1317–1329.

Fisher, I. 1986. Pyrite formation in bioturbated clays from the Jurassic of Britain. *Geochimica Cosmochimica Acta,* **50,** 517–523.

Fox, J.S. & Videtich, P.E. 1997. Revised estimate of $\delta^{34}S$ for marine sulfates from the Upper Ordovician: data from the Willistone Basin, north Dakota, USA. *Applied Geochemistry,* **12,** 97–103.

German, C.R. & Elderfield, H. 1990. Application of the Ce anomaly as a paleoredox indicator: the ground rules. *Paleoceanography,* **5,** 823–833.

Hall, A.J., Boyce, A.J., Fallick, A.E. & Hamilton, P.J. 1991. Isotopic evidence of the depositional environment of Late Proterozoic stratiform barite mineralistion, Aberfeldy, Scotland. *Chemical Geology,* **87,** 99–114.

Holland, H.D. 1984. *The chemical evolution of the atmosphere and oceans*. Princeton University Press. Princeton, New Jersey.

Holser, W.T. 1977. Catastrophic chemical events in the history of the ocean. *Nature,* **267,** 403–408.

—— 1997. Evaluation of the application of rare-earth elements to paleoceanography. *Palaegeography, Palaeoclimatology and Palaeoecology,* **132,** 309–323.

Houghton, M.L. 1980. *Geochemistry of the Proterozoic Hormuz evaporites, Southern Iran*. MSc Thesis, Oregon.

Hsü, K.J., Oberhänsli, H., Gao, J., Sun, S., Chen, H. & Krähenbühl, U. 1985. 'Strangelove Ocean' before the Cambrian explosion. *Nature,* **316,** 809–811.

Ilyin, A.V. 1998. Rare-earth geochemistry of 'old' phosphorites and probability of syngenetic precipitation and accumulation and phosphate. *Chemical Geology,* **144,** 243–256.

Jarvis, I., Burnett, W., Nathan, Y., Almbaydin, F.S.M., Attia, A.K.M., Castro, L.N., Flicoteaux, R., Hilmy, M.E., Husain, V., Qutawnah, A.A., Serjani, A. & Zanin, Y.N. 1994. Phosphorite geochemistry: State-of-the-art and environmental concerns. *Eclogae Geologicae Helveticae,* **87,** 3, 643–700.

Jensen, S., Grant, S.W., Kaufman, A.J. & Corsetti, F.A. 1996. Afterthoughts on chemostratigraphy of Neoproterozoic-Cambrian units, White-Inyo Region, E. California and W. Nevada: Implications for global correlation and faunal distribution: discussion and reply. *Palaios ,* **50,** 77–86.

Kampschulte, A. & Strauss, H. 1996. The Sulfur Isotopic Composition of Jurassic and Cretaceous Seawater as Deduced From Trace Sulfate in Belemnites. Goldschmidt-Conference, Heidelberg, 31.3.–4.4.96. *Journal of Conference Abstracts,* **1,** 303.

Kampschulte, A. & Strauss, H. 1998. The isotopic composition of trace sulphates in Palaeozoic biogenic carbonates: Implications for coeval seawater and geochemical cycles. *Mineralogical Magazine,* **62A,** 744–745.

Kaufman, A.J. & Knoll, A.H. 1995. Neoproterozoic variations in the C-isotope composition of seawater: stratigraphic and biogeochemical implications. *Precambrian Research,* **73,** 27–49.

Kirschvink, J.L., Margaritz, M., Ripperdan, R.L., Zhuravlev, A.Y. & Rozanov, A.Y. 1991. The Precambrian-Cambrian boundary problem 2: Magnetostratigraphic and carbon isotope correlations for Tommotian and Atdabanian time between Siberia, Morocco and South China. *GSA Today,* **1,** 69–91.

Knoll, A.H., Kaufman, A.J., Semikhatov, M.A. & Grotzinger, J.P. 1995. Sizing up the sub-Tommotian unconformity in Siberia. *Geology,* **23,** 12, 1139–1143.

Lambert, I.B., Walter, M.R., Zang, Wenlong, Lu, S. & Ma, G. 1987. Palaoenvironment and carbon isotope stratigraphy of Upper Proterozoic carbonates of the Yangtze Platform. *Nature,* **325,** 140–142.

Landing, E. 1994. Precambrian-Cambrian boundary global stratotype ratified and a new perspective of Cambrian time. *Geology,* **22,** 179–182.

Li, R. 1991. Trace fossils and the Sinian-Cambrian boundary in the Meishucun sections, eastern Yunnan, China and their relations to small shelly fossils. *Geological Review,* **37,** 214–220.

Lindsay, J.F., Brasier, M.D., Dorjnamjaa, D., Goldring, R., Kruse, P.D. & Wood, R.A. 1996. Facies and sequence controls on the appearance of the Cambrian biota in southwestern Mongolia: implications for the Precambrian-Cambrian boundary. *Geological Magazine,* **133,** 417–428.

Logan, G.A., Hayes, J.M., Hieshima, G.B. & Summons, R.E. 1995. Terminal Proterozoic reorganization of biogeochemical cycles. *Nature,* **376,** 53–56.

Louie, P.K.K., Bottrell, S.H., Timpe, R.C., Hawthorne, S.B. & Miller, D.J. 1995. An improved method for extracting sulphate from bituminous coals using formic acid. *Fuel,* **74,** 1480–1484.

Luo, H. 1980. On the Sinian-Cambrian boundary of Meishucun and Wanjiawan, Jinning County, Yunnan. *Acta Geologica Sinica,* **2,** 95–111 [in Chinese].

——, Jiang, Z., Wu, X., Lin, O., Song, X. & Xue, X. 1992. A further research on the Precambrian-Cambrian boundary at Meishucun Section of Jinning, Yunnan, China. *Acta Geologica Sinica* (English edition), **5,** 197–206.

——, ——, ——, Song, X., Lin, O., Xing., Y., Liu, G., Zhang, S. & Tao, Y. 1984. *Sinian-Cambrian boundary stratotype section at Meishucun, Jinning, Yunnan, China*. People's Publishing House, Yunnan, China.

Mattes, B.W. & Conway Morris, S. 1990. Carbonate/evaporite deposition in the Late Precambrian–Early Cambrian Ara Formation of Southern Oman. *In*: Robertson, A.H.F., Searle, M.P. & Ries, A.C. (eds) *The Geology and Tectonics of the Oman Mountains*. Geological Socety, London, Special Publication, **49,** 617–636.

McArthur, J.M. & Walsh, J.N. 1984. Rare-earth geochemistry of phosphorites. *Chemical Geology,* **47,** 191–220.

——, Benmore, R.A., Coleman, M.L., Soldi, C., Yeh, H-W. & O'Brien, G.W. 1986. Stable isotopic characterisation of francolite formation. *Earth and Planetary Science Letters,* **77,** 20–34.

Misi, A. & Kyle, J.R. 1994. Upper Proterozoic carbonate stratigraphy, diagenesis and stromatolitic phosphorite formation, Irece Basin, Bahia, Brazil. *Journal of Sedimentary Research,* **A64,** 2, 299–310.

—— & Veizer, J. 1998. Neoproterozoic carbonate sequences of the Una Group, Irece Basin: chemostratigraphy, age and correlations. *Precambrian Research,* **89,** 87–100.

Nakai, N. & Jensen, M.L. 1964. The kinetic isotope effect in the bacterial reduction and oxidation of sulphur. *Geochimica et Cosmochimica Acta,* **28,** 1893–1912.

Narbonne, G.M., Myrow, P.M., Landing, E. & Anderson, M.M. 1987. A candidate stratotype for the Precambrian-Cambrian boundary, Fortune Head, Burin Peninsula, southeastern Newfoundland. *Canadian Journal of Earth Sciences,* **24,** 1277–1293.

Pisarchik, Y.K. & Golubchina, M.N. 1975. Sulfur isotope composition for Cambrian calcium sulfates from the Siberian Platform. *Geochemistry International,* **8,** 227–230.

——, —— & Toksubayev, A.I. 1977. Isotopic composition of sulfur in calcium sulfates from the Upper Lena Formation (Siberian Platform). *Geochemistry International,* **4,** 182–185.

Poulton, S.W., Bottrell, S.H. & Underwood, C.J. 1998. Porewater sulphur geochemistry and fossil preservation during phosphate diagenesis in a Lower Cretaceous shelf mudstone. *Sedimentology,* **45,** 875–887.

Qian, Y. & Bengston, S. 1989. Palaeontology and biostratigraphy of the Early Cambrian Meishucunian Stage in Yunnan Province, South China. *Fossils and Strata,* **24,** 1–156.

Ross, G.M., Bloch, J.D. & Krouse, H.R. 1995. Neoproterozoic strata of the southern Canadian Cordillera and the isotopic evolution of seawater sulfate. *Precambrian Research,* **73,** 71–99.

Rozanov, A.Y. 1984. The Precambrian-Cambrian boundary in Siberia. *Episodes,* **7,** 1, 20–24.

Sambridge, M.S. & Compston, W. 1994. Mixture modelling of multi-component data sets with application to ion-probe zircon ages. *Earth and Planetary Science Letters,* **128,** 373–390.

Shen, Y., Zaho, R., Chu, X. & Lei, J. 1998. The carbon and sulfur isotope signatures in the Precambrian-Cambrian transition series of the Yangze Platform. *Precambrian Research,* **89,** 77–86.

Shields, G.A. 1996. *Event stratigraphy around the Precambrian/Cambrian boundary with special emphasis on western Mongolian and South China*. Doctoral thesis, ETH Zurich.

Shields, G.A., Stille, P. & Brasier, M.D. 1999. Isotopic records across two phosphorite giant episodes compared: the Precambrian–Cambrian and the late Cretaceous-recent. *In*: Glenn, C., Lucas, J. & Prévot-Lucas, L. (eds) *Marine authigenesis: From Global to Microbial*. SEPM special volume. Tulsa, Oklahoma, USA, in press.

——, ——, —— & Atudorei, N.-V. 1997. Stratified oceans and oxygenation of the late Precambrian environment: a post glacial geochemical record from the Neoproterozoic of W Mongolia. *Terra Nova,* **9,** 218–222.

Siegmund, H. 1995. *Fazies und Genese unterkambrischer Phosphorite und mariner Sedimente der Yangtze Plattform, SüdChina*. Berliner geowissenschaftliche Abhandlungen, **A173,** Berlin.

—— & Erdtmann, B.-D. 1995. Lower Cambrian phosphorites of south China: Microfacies and genetic interpretation. *Zentralblatt für Geologie und Paläontologie,* Teil 1, **1/2,** 257–270.

Smirnov, A.I., Ivnitzkaya, R.B. & Zalavina, T.P. 1962. Experimental data on the possibility of the chemical precipitation of phosphate from seawater. *In*: *Geology of Phosphorite deposits*. State Scientific Research Institute for the chemistry of raw materials, **7,** 289–302.

Strauss, H. 1993. The sulfur isotopic record of Precambrian sulfates: new data and a critical evaluation of the existing record. *Precambrian Research,* **63,** 225–246.

—— 1996. The Sulfur Isotopic Composition of Seawater as deduced From Trace Sulfates in Carbonates. Goldschmidt-Conference, Heidelberg, 31.3.–4.4.96. *Journal of Conference Abstracts,* **1,** 601.

—— & Banerjee, D.M. 1998. The Sulfur isotopic composition of Neoproterozoic to early Cambrian seawater—evidence from the cyclic Hanseran evaporites, NW India. *Mineralogical Magazine,* **62A,** 1467–1468.

Thode, H.G. & Monster, J. 1965. Sulfur-isotope geochemistry of petroleum, evaporites and ancient seas. *In*: *Fluids in subsurface environments—a symposium*. American Association of Petroleum Geologists Memoirs, **4,** 367–377.

Wang, Z. & Li, G. 1991. Barite and witherite deposits in Lower Cambrian shales of South China: Stratigraphic distribution and geochemical characterisation. *Economic Geology,* **86,** 354–363.

Xing, Y., Luo, H., Jiang, Z. & Zhang, S. 1991. A candidate global stratotype section and point for the Precambrian-Cambrian boundary at Meishucun, Yunnan, China. *Journal of China University of Geosciences,* **2,** 1, 47–57.

Yanagisawa, F. & Sakai, H. 1983. Thermal decomposition of barium sulfate-vanadium pentaoxide-silica glass mixtures for preparation of sulfur dioxide in sulfur isotope ratio measurements. *Analytical Chemistry,* **55,** 985–987.

Received 2 November 1998; revised typescript accepted 15 February 1999.
Scientific editing by Ian Fairchild.